PCT WORLD INTELLECTUAL PROPERTY ORGANIZATION
International Bureau

INTERNATIONAL APPLICATION PUBLISHED UNDER THE PATENT COOPERATION TREATY (PCT)

(51) International Patent Classification 6 : A61B 5/05

A1

(11) International Publication Number: WO 98/02091

(43) International Publication Date: 22 January 1998 (22.01.98)

(21) International Application Number: PCT/US97/11592

(22) International Filing Date: 11 July 1997 (11.07.97)

(30) Priority Data:
60/021,588 11 July 1996 (11.07.96) US

(71) Applicant: THE BOARD OF TRUSTEES OF THE LELAND STANFORD JUNIOR UNIVERSITY [US/US]; Suite 350, 900 Welch Road, Palo Alto, CA 94304 (US).

(72) Inventors: MURPHY, Martin, J.; 1777 Walnut Street, San Carlos, CA 94070 (US). COX, Richard, S.; 35 Corto Lane, Woodside, CA 94062 (US).

(74) Agent: McFARLANE, Thomas, J.; 426 Lowell Avenue, Palo Alto, CA 94301 (US).

(81) Designated States: AU, CA, JP, European patent (AT, BE, CH, DE, DK, ES, FI, FR, GB, GR, IE, IT, LU, MC, NL, PT, SE).

Published
With international search report.
Before the expiration of the time limit for amending the claims and to be republished in the event of the receipt of amendments.

(54) Title: HIGH-SPEED INTER-MODALITY IMAGE REGISTRATION VIA ITERATIVE FEATURE MATCHING

(57) Abstract

This invention describes a method for aligning radiation therapy beams with a treatment target of a patient. Diagnostic computer tomography scanning is used to map the treatment target in the patient's anatomy and to aid physicians in deciding where to aim the radiation therapy beams. Digitally reconstructed radiographs are generated from an intermediate 3-D image produced from the CT scans. These DRRs are compared with x-ray images taken of the treatment target's position taken at the time of treatment. A transformation equation is used to compare the DRRs and the x-ray images. A minimization equation is used to determine the similarity between the two sets of images. If the difference between the two sets fall below a determined minimum value, then the position of the treatment target is deemed correct and the radiation therapy begins. If the difference does not fall below the determined minimum value, then either the radiation beams or the treatment target is adjusted and the process is repeated. This procedure may be used many times in the course of a single treatment session, depending on the movement of the patient.

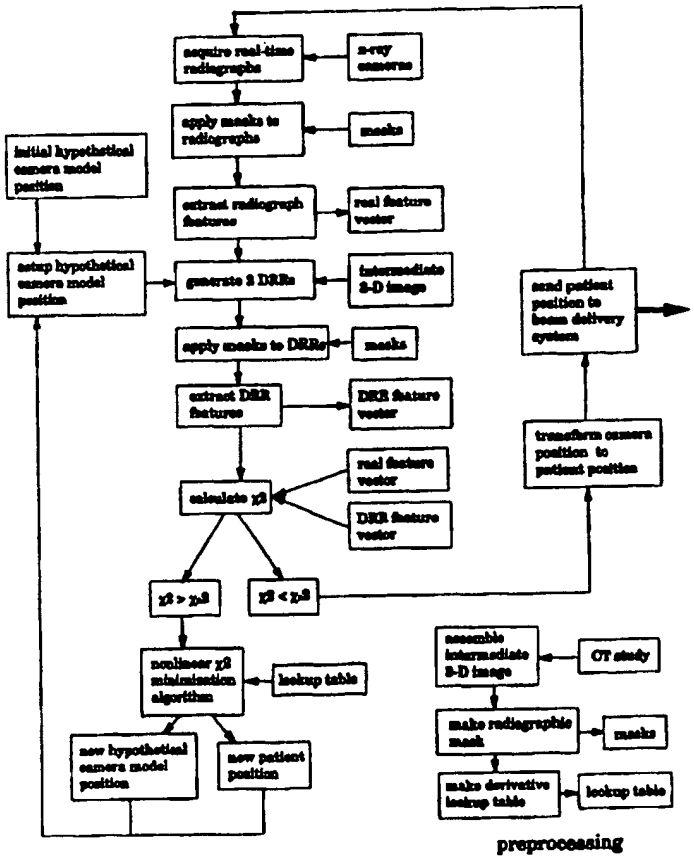

FOR THE PURPOSES OF INFORMATION ONLY

Codes used to identify States party to the PCT on the front pages of pamphlets publishing international applications under the PCT.

AL	Albania	ES	Spain	LS	Lesotho	SI	Slovenia
AM	Armenia	FI	Finland	LT	Lithuania	SK	Slovakia
AT	Austria	FR	France	LU	Luxembourg	SN	Senegal
AU	Australia	GA	Gabon	LV	Latvia	SZ	Swaziland
AZ	Azerbaijan	GB	United Kingdom	MC	Monaco	TD	Chad
BA	Bosnia and Herzegovina	GE	Georgia	MD	Republic of Moldova	TG	Togo
BB	Barbados	GH	Ghana	MG	Madagascar	TJ	Tajikistan
BE	Belgium	GN	Guinea	MK	The former Yugoslav Republic of Macedonia	TM	Turkmenistan
BF	Burkina Faso	GR	Greece			TR	Turkey
BG	Bulgaria	HU	Hungary	ML	Mali	TT	Trinidad and Tobago
BJ	Benin	IE	Ireland	MN	Mongolia	UA	Ukraine
BR	Brazil	IL	Israel	MR	Mauritania	UG	Uganda
BY	Belarus	IS	Iceland	MW	Malawi	US	United States of America
CA	Canada	IT	Italy	MX	Mexico	UZ	Uzbekistan
CF	Central African Republic	JP	Japan	NE	Niger	VN	Viet Nam
CG	Congo	KE	Kenya	NL	Netherlands	YU	Yugoslavia
CH	Switzerland	KG	Kyrgyzstan	NO	Norway	ZW	Zimbabwe
CI	Côte d'Ivoire	KP	Democratic People's Republic of Korea	NZ	New Zealand		
CM	Cameroon			PL	Poland		
CN	China	KR	Republic of Korea	PT	Portugal		
CU	Cuba	KZ	Kazakstan	RO	Romania		
CZ	Czech Republic	LC	Saint Lucia	RU	Russian Federation		
DE	Germany	LI	Liechtenstein	SD	Sudan		
DK	Denmark	LK	Sri Lanka	SE	Sweden		
EE	Estonia	LR	Liberia	SG	Singapore		

High-Speed Inter-Modality Image Registration Via Iterative Feature Matching

RELATED APPLICATION INFORMATION

This application claims priority from U.S. Provisional Application No. 60/021,588 entitled "HIGH-SPEED INTER-MODALITY IMAGE REGISTRATION VIA ITERATIVE FEATURE MATCHING" filed July 11, 1996, which is herein incorporated by reference.

FIELD OF THE INVENTION

This invention relates to the field of medical imaging. More particularly, it relates to a real-time method of positioning therapeutic radiation beams with respect to a target area within a patient.

BACKGROUND OF THE INVENTION

Radiation therapy is often used to treat cancerous tumors within a patient's body. An early diagnostic session is conducted where the physician uses an imaging technique, such as computed tomography (CT) scanning or magnetic resonance imaging (MRI) to study the target area. He or she then decides the ideal placement and volume of the radiation beam(s) with respect to the target area. During the actual treatment, the radiation beams are focused directly at the target area, using the diagnostic studies as a position reference. Precise positioning of the radiation beams insures that most of the radiation contacts the target cells, while also insuring that the healthy cells surrounding the target cells are not affected. Unfortunately, it is often difficult to be certain that radiation beams are optimally positioned with

respect to target cells. Often, a smaller total dose of radiation must be used in order to reduce the possibility of damage to healthy cells. The consequence, however, is that the radiation treatment becomes less effective.

In addition, radiotherapy often requires a patient to return for treatment over the course of several days. Repositioning a patient precisely each time can be time-consuming and frustrating.

Over the past decade, many methods have been devised to improve the alignment of radiation beams with the target area of a patient. An early method involves a rigid frame to physically hold in place the part of the patient's body to be treated. In one embodiment for treatment of target areas within a patient's skull, the frame is attached to a floorstand mounted in a Linac (linear accelerator) floor turret. This method is considered generally reliable and accurate, as it fixes the target area rather precisely with respect to the radiation beams. Unfortunately, due to the nature of the frame, it also greatly limits accessibility to the patient's skull. Target areas may be located in the skull where the Linac radiation beams cannot reach. In addition, it is extremely uncomfortable for the patient, who must remain in an awkward position for long periods of time.

Another method involves invasive techniques. Patent No. 5,097,839 by Allen describes fiducial implants attached in a pattern to a patient's skull bones, underneath the skin. These implants are then used as fixed references when aligning radiation beams with the target area. These implants are an improvement over rigid frames in that they allow all target areas within a skull to be reached. However, because inserting the fiducial implants into the patient is a surgical procedure itself, the patient must often wait for several days until the radiation treatment. During this time, the target area may grow or otherwise change in shape, rendering inaccurate the early diagnostic analyses taken when the fiducial implants were put in

place. In addition, the implants are often disfiguring and painful to the patient.

Another type of invasive technique involves placing tattoos on the patient's skin where the radiation beams are to enter. Although this is less intrusive than the fiducial implants, it has many of the same problems, such as the patient having to wait several days from the time of the tattoo procedure until the radiation treatment, thus giving time for the target area to grow or change shape. In addition, given the nature of tattoos, it is possible they may also change shape.

More recently, non-invasive, non-disfiguring alignment systems have been developed. These typically use signal processing to convert the CT or MRI data of the position of the patient in the diagnostic setting to the position of the patient in the treatment setting. Many of these systems require a large amount of preprocessing, whereby data generated from the diagnostic scan is gathered and manipulated until it is usable in the treatment setting. The preprocessing step can take several days. During treatment, real time images are compared with the preprocessing data and the patient or the radiation therapy beams are adjusted accordingly. Oftentimes, manual adjustment is necessary. Three degrees of freedom, corresponding to one plane, are typically allowed. The patient has greater freedom of movement than in the previously described techniques, but his movement is still confined. These systems are generally accurate, and painless for the patient.

Patent No. 5,295,200 by Boyer et al. describes a method of aligning radiation therapy beams using the Fast Fourier Transform (FFT) to compare the position of diagnostic images with the position of treatment images. In this invention, a large amount of complex data must be gathered and processed prior to treatment. Reference images collected during the diagnostic study are later used to position the patient during treatment.

Patent No. 5,531,520 by Grimson et al. describes a method of image registration that takes into consideration patient movement within six degrees of freedom. It employs lasers to determine patient position and as such is confined to surface images. Thus, treatment beams must be based relative to tattoos or other markers on a patient's skin, which have the problems mentioned above.

These existing alignment methods require an extensive amount of time to process complex diagnostic data, usually restrict accuracy to three degrees of freedom, limit patient movement, and make adjustment of either the treatment beams or the patient difficult. In addition, they are unable to generate instant reference images with which to compare the present position of a patient. They also require manual operations to supplement automatic procedures.

OBJECTS AND ADVANTAGES OF THE INVENTION

Accordingly, it is a primary object of the present invention to provide a wholly automatic method of aligning radiation therapy beams with the treatment target of a patient. It is another object of the invention to provide such a method by making use of radiographic techniques. Yet another object of the invention is to decrease the time required for the preprocessing step, as well as reduce the complexity of data manipulation. A further object of this invention is to generate instant reference images derived from the diagnostic study with which to compare the present position of the treatment target. Another object of the invention is to allow a patient to move around freely during treatment. A sixth object of the invention is to measure patient movement within six degrees of freedom. A seventh object of the invention is to provide continuous adjustment of radiation therapy beams to improve precision during the course of treatment. A final object of this invention is to accommodate both diagnostic imaging and treatment of a patient in the same day.

SUMMARY OF THE INVENTION

These objects and advantages are attained by the present invention. This method begins with a diagnostic computed tomographic (CT) scan of the treatment target of a patient. The information from the CT scan is used to generate an intermediate 3-D image. This intermediate 3-D image will eventually be moved or rotated to mimic the position of the treatment target. During treatment, the position of the treatment target in relation to the radiation therapy beams is recorded using at least two x-ray cameras. Thus, both translational and rotational information is received. The treatment images are then processed to produce a feature vector, which is specific for those set of images and thus the position of the treatment target.

Using the intermediate 3-D image generated during the diagnostic stage, at least two digitally reconstructed radiographs (DRRs) are produced. These radiographs are wholly artificial constructs that are judged to be similar to the treatment images. These DRRs are also processed to produce a feature vector. The difference between the two feature vectors is then calculated using a mathematical equation, for example chi squared. If the difference falls below a minimum allowable value, then the position of the treatment target is deemed accurate enough to begin radiation therapy. However, if the difference does not fall below the minimum allowable value, then the intermediate 3-D image is iteratively moved within six degrees of freedom until successive DRRs produce an acceptable minimum difference with respect to the treatment images. Data from the repositioned intermediate 3-D image is used to adjust either the patient or the radiation therapy beams, thus achieving accurate alignment of the radiation beams and the treatment target.

DESCRIPTION OF THE FIGURES

Fig. **1** is a flow chart illustrating the operation of the invention.

Fig. **2** shows a radiograph produced from a patient with a brain tumor.

Fig. **3** is a diagram of the apparatus, consisting of a Cyberknife connected to a computer system.

Fig. **4** is a diagram showing the diagnostic coordinate system.

Fig. **5** is a diagram showing the treatment coordinate system.

Fig. **6** is a diagram showing the three translational degrees of freedom in the preferred embodiment.

Fig. **7** is a diagram showing the three rotational degrees of freedom in the preferred embodiment.

Fig. **8** is a diagram illustrating the projection geometry for generating two digitally reconstructed radiographs (DRRs) from the intermediate 3-D image using a hypothetical camera model.

Fig. **9** shows a fluoroscopic image of an anthropomorphic phantom, a DRR of said anthropomorphic phantom, and a DRR marked with key pixels to locate anatomical edge features.

Fig. **10** contains graphs showing the empirical results for determining (x, y, z) translations, (α, β, γ) rotations one axis at a time, and composite (α, β) rotations for an anthropomorphic phantom.

Fig. **11** is a table showing the standard deviation of errors in measuring translations and rotations of the anthropomorphic phantom.

Fig. **12** is a graph illustrating the distribution of rotation measurement errors for the empirical tests. The distribution is approximately Gaussian with zero mean.

Fig. **13** is a graph showing the distribution of $\chi 2$ from the empirical tests.

Fig. **14** is a graph showing the correlation between $\chi 2$ and the errors in angle measurements from the empirical tests.

Fig. **15** is a graph showing the correlation between $\chi 2$ and the rotation angles around each axis from the empirical tests.

DETAILED DESCRIPTION

For illustrative purposes, the method of the invention is described for use with the Cyberknife, as shown in Fig. **3**, and a patient **30** with a brain tumor **32**, as shown in Fig. **2**. Please note the method of this invention is not confined for use with the Cyberknife. In the preprocessing step, patient **30** undergoes a computed tomography (CT) scan of his skull. The CT scans are used to assemble an intermediate 3-D image **54**, as shown in Fig. **8**. Intermediate 3-D image **54** can be moved and rotated along both translational axes **50** and rotational axes **52** in the diagnostic coordinate system, as shown in Figs. **6** and **7**. In this representation, translational axes **50** are represented by dx, dy, and dz, while the rotational axes **52** are represented by α, β, γ. Thus up to six degrees of freedom of movement are allowed. Intermediate 3-D image **54** may consist solely of computer script within a computer or system of computers **44** or it may be visualized on a monitor.

In the preferred embodiment, intermediate 3-D image **54** is used to generate a set of at least two digitally reconstructed radiographs (DRRs) **56**, as shown in Fig. **8**. DRRs **56** are artificial 2-D images that show how intermediate 3-D image **54** would appear from different angles using a hypothetical camera model **58**. Each DRR **56** of a set represents one hypothetical camera angle. These DRRs **56** can then be masked to isolate key pixels associated with anatomical edge features **64**, as shown in Fig. **9**. Where a complete image **60** would have 40,000 pixels, for example, a masked image **62** typically has 1,000 to 4,000 key pixels **64**.

The set of masked DRRs **62** may then be used to generate a lookup table. The lookup table provides the

first derivatives of said translational and rotational measurements of intermediate 3-D image **54**. These calculations can be used later during treatment to match the actual patient images with intermediate 3-D image **54**. The preprocessing procedure as described above requires about 20 seconds on a computer or computer systems **44** with 200 MHz processors.

During treatment, the patient is placed within the view of at least two radiographic cameras **42**, in a position approximating his position during the diagnostic scan. The patient has complete freedom of movement, as all possible positions can be defined within six degrees of freedom using translational axes **50** and rotational axes **52**, as shown in Figs. **6** and **7**. Translational axes **50** and rotational axes **52** of the treatment coordinate system, as shown in Fig. **5**, are defined in the same manner as translational axes **50** and rotational axes **52** of the diagnostic coordinate system, as shown in Fig. **4**. (On the Cyberknife, patient **30** has two x-ray cameras **42** and screens **36**, which produce real-time radiographs **31** of treatment target **32**). These real-time radiographs **31** may then be processed in the same manner as DRRs **56**. Real-time radiographs **31** are masked to isolate key pixels associated with anatomical edge features **64**. Masked real-time radiographs **31** are used to produce a first feature vector, which specifically identifies the position and orientation of treatment target **32** within the treatment coordinate system, as shown in Fig. **5**, at the time real-time radiographs **31** were taken.

Next, intermediate 3-D image **54** is manipulated until its position emulates the position and orientation of treatment target **32**. New DRRs **56** are then generated from intermediate 3-D image **54**, as shown in Fig. **8**. These DRRs **56** are masked to isolate the same key pixels **64** as in real-time radiographs **31** and processed to produce a second feature vector, which specifically identifies the position and orientation of the treatment target of intermediate 3-D

image **54** within the diagnostic coordinate system, as shown in Fig. **4**.

The two feature vectors are then compared using a mathematical equation, for example the chi squared statistic. If treatment target **32** of patient **30** is positioned in the treatment coordinate system, as shown in Fig. **5**, in precisely the same way as intermediate 3-D image **54** is positioned in the diagnostic coordinate system, as shown in Fig. **4**, then the difference between the two feature vectors, or χ^2, will be less than a designated minimum value. The system has then completed its determination of treatment target **32** position and orientation. This information is passed on to the beam delivery system **40** (e.g. the Cyberknife) and the radiation therapy beams **38** are allowed to operate.

If, however, treatment target **32** is not positioned in the same position and orientation as in the diagnostic coordinate system, the two feature vectors will exhibit χ^2 greater than the designated minimum value. In this case, the system moves to the χ^2 minimization step. The χ^2 minimization process searches for a match between real-time radiographs **31** and DRRs **56** by iteratively varying the position and orientation of intermediate 3-D image **54** with respect to hypothetical camera model **56**. For a radiographic imaging system consisting of at least two CCD fluoroscopes, hypothetical camera model **58** is a multi-parameter function which maps the CCD image plane to the fluoroscope screen, and the fluoroscope screen to the treatment coordinate system, as shown in Fig. **5**. It accounts for magnification, relative positioning of the two fluoroscopes in the treatment room coordinate system, tilt of the image planes with respect to the fluoroscope screens (in three independent directions), and radial (spherical) distortion of the lens system. Radial distortion is modeled by the factor:

$$x' = x / (1 + \lambda R^2)$$
$$y' = y / (1 + \lambda R^2)$$

where x and y are the pixel coordinates on the CCD image plane, x' and y' are the corresponding coordinates on the fluoroscope screen, $R^2 = (x^2 + y^2)$, and λ is a free parameter that is determined when hypothetical camera model **58** is calibrated.

The parameters of hypothetical camera model **58** are determined by fitting DRRs **56** of a calibration phantom to actual radiographs **31** of the phantom, using the same χ^2 minimization process as for patient position measurements. The residual errors in this calibration-fitting process are spatially random and on the order of the image pixel dimensions, indicating that there is no significant distortion left unaccounted for by the model.

The various positions of the treatment target are emulated in DRRs **56** by changing the point of view of hypothetical camera model **58** with respect to intermediate 3-D image **54**. This movement is achieved by use of the lookup table created in the preprocessing step, as described above. The process continues until the difference between the two feature vectors falls below the designated minimum value. At this point, the new coordinates of hypothetical camera model **58** in the diagnostic coordinate system are translated into coordinates for the treatment coordinate system. This information is sent to beam delivery system **40** and radiation therapy beams **38** are realigned. It is also possible to reposition patient **30**. Radiation therapy beams **38** are then allowed to operate.

Translation of intermediate 3-D image **54** rotation geometry into the treatment target geometry is accomplished most effectively via an Eulerian (body-fixed) rotation convention. The Eulerian convention properly represents the fact that patient's rotational axes **52** are fixed in anatomy and not in an external reference frame. On the other hand, mechanical beam and patient alignment systems can measure angles in the space-fixed (α, β, γ) convention illustrated in Fig. **10**. To relate space-fixed rotations in

(α, β, γ) with the rotations deduced by the image registration algorithm requires that the Eulerian DRR rotations be inverted to correspond to rotations of the object rather than hypothetical camera model **58** (bearing in mind that sequential rotations do not commute) and then transformed to the space-fixed rotation convention. This transformation is summarized below.

Let us designate treatment target **32** in the skull of patient **30** by the vector **x** in the space-fixed camera coordinate system. When treatment target **32** rotates through the angles (α, β, γ), its coordinates in the fixed frame become

$$\mathbf{x}'' = [\Lambda\gamma][\Lambda\beta][\Lambda\alpha]\mathbf{x}$$

where the rotation matrices are:

$$[\Lambda\gamma] = \begin{matrix} 1 & 0 & 0 \\ 0 & \cos\alpha & \sin\alpha \\ 0 & -\sin\alpha & \cos\alpha \end{matrix}$$

$$[\Lambda\beta] = \begin{matrix} \cos\beta & 0 & \sin\beta \\ 0 & 1 & 0 \\ -\sin\beta & 0 & \cos\beta \end{matrix}$$

$$[\Lambda\alpha] = \begin{matrix} \cos\gamma & -\sin\gamma & 0 \\ \sin\gamma & \cos\gamma & 0 \\ 0 & 0 & 1 \end{matrix}$$

This convention locates points in the anatomy of patient **30** in the fixed treatment coordinate frame that beam delivery system **40** refers to in directing treatment beam **38**.

The DRR ray-tracing process works most effectively in a coordinate system fixed to the image plane in hypothetical camera model **58**. The image plane of hypothetical camera model **58** is positioned within the diagnostic coordinate system, relative to intermediate 3-D

image **54**, through the three Eulerian rotations $(\phi_0, \theta_0, \psi_0)$. Rotations of the patient's anatomy with respect to x-ray cameras **42** can then be represented in the DRR process by moving the image plane of hypothetical camera model **58** through $(\phi_0, \theta_0, \psi_0)$ to the perturbed orientation $(\phi_0 + d\phi, \theta_0 + d\theta, \psi_0 + d\psi)$. If a point in the patient's anatomy is located by the vector **X'** in the coordinate frame fixed to the image plane, then **X** and **X'** are related according to the transformation:

$$\mathbf{X}'' = [\Lambda_\phi][\Lambda_\theta][\Lambda_\psi]\mathbf{X}$$

where the rotation matrices are:

$$[\Lambda_\phi] = \begin{matrix} 1 & 0 & 0 \\ 0 & \cos\phi & \sin\phi \\ 0 & -\sin\phi & \cos\phi \end{matrix}$$

$$[\Lambda_\theta] = \begin{matrix} \cos\theta & 0 & \sin\theta \\ 0 & 1 & 0 \\ -\sin\theta & 0 & \cos\theta \end{matrix}$$

$$[\Lambda_\psi] = \begin{matrix} \cos\psi & -\sin\psi & 0 \\ \sin\psi & \cos\psi & 0 \\ 0 & 0 & 1 \end{matrix}$$

Let $[\mathbf{E}_0] = [\Lambda_\phi][\Lambda_\theta][\Lambda_\psi]$ define the complete Eulerian rotation matrix for angles $(\phi_0, \theta_0, \psi_0)$ and $[\mathbf{E}_0 + d\mathbf{E}]$ define the complete rotation matrix for rotations $(\phi_0 + d\phi, \theta_0 + d\theta, \psi_0 + d\psi)$. The inverse transformtion is $[\mathbf{E}^{-1}] = [\Lambda_{-\phi}][\Lambda_{-\theta}][\Lambda_{-\psi}]$. Following this convention, the vector locating the point **X"** in the treatment coordinate frame after a rigid-body rotation $(d\phi, d\theta, d\psi)$ that is modeled by the rotation of hypothetical camera model **58** is given by:

$$\mathbf{X}'' = [\mathbf{E}_0^{-1}][\mathbf{E}_0 + d\mathbf{E}]\mathbf{X}.$$

From this, the relationship between the space-fixed rotations (α, β, γ) and the body-fixed Eulerian rotations $(d\phi, d\theta, d\psi)$ is given by:

$$[\mathbf{E}_0^{-1}][\mathbf{E}_0 + d\mathbf{E}] = [\Lambda\gamma][\Lambda\beta][\Lambda\alpha]$$

EMPIRICAL TESTS

The reduction of this method to practice has been demonstrated in the following tests. In the tests, the precision of measuring actual phantom rotations will be reported in (α, β, γ), while numerical simulations of rotation measurement will be reported in (ϕ, θ, ψ) Eulerian angles.

In the tests, an anthropomorphic skull phantom was set up on the treatment couch, with the inferior/superior axis along the x-ray camera x-axis, as it would be for a typical patient. The phantom's anterior direction was in the positive z direction. The three axes of rotation in the test setup corresponded to the space-fixed angles (α, β, γ), as defined in Fig. 7. A tiltmeter measured angles (α, β) relative to gravity and was calibrated on a milling machine's rotary table. The resulting calibration was accurate to better than 0.1 degrees. The remaining translational and rotational degrees of freedom were measured mechanically and had precisions of 0.25 mm and 0.25 degrees, respectively.

The phantom was imaged in a CT study of 74 slices 3.0 mm thick, with each image having 512 x 512 pixels 0.49 mm on a side. The treatment room imaging system operated at 100 kV and 25 mA. The radiographs were 200 x 200 pixels, with each pixel 1.30 mm on a side.

The phantom was moved step-by-step through motions along and around each axis separately and in composite multi-axis rotations. At each step, the imaging system acquired radiographs and the algorithm computed the phantom position and orientation relative to the CT study. The correspondence between the measured and actual change in

position was recorded for each individual degree of freedom. For each test position, the minimum value of χ^2 at convergence was recorded.

Fig. **10** illustrates the results for determining translations and rotations empirically. This figure displays the known translations and rotations along the abscissa and the deduced translations and rotations along the ordinate. The figure shows data for rotations (α, β, γ) around one axis at a time, and data for composite rotations in which α and β were varied simultaneously. The individual β and γ rotations each correspond to a composite rotation of φ and ψ in the Eulerian system used to model phantom position in the DRRs. The composite rotations involved all three Eulerian angles.

The deduced versus actual translations and rotations should follow straight lines of slope equal to one. The data displayed in the figures were fit to straight lines, in one case fixing the slope to one, and in the other case allowing the slope to be a free parameter. The variance of the individual points about the fitted line is the standard deviation. The results of analyzing the data via straight line fits are summarized in Fig. **11**.

Fig. **12** plots the frequency distribution of angle measurement errors. This distribution has an approximately Gaussian shape with zero mean, which is consistent with the conclusion that the process is not making systematic errors in determining the phantom position. The frequency distribution for χ^2 at convergence is plotted in Fig. **13**. This distribution has the basic functional form of a χ^2 distribution for fits to data with randomly distributed statistical fluctuations. This again supports the conclusion that the process of extracting the image moments and edge coordinates that are fit by χ^2 minimization is not making systematically biased determinations of the image features.

Fig. **14** illustrates the correspondence between the measurement error for each rotational component and the value of χ^2 at convergence The relationship is

uncorrelated for values of χ^2 less than one and rotation errors less than about one degree. This is consistent with the supposition that once the position determination has gotten close, the minimization routine encounters a χ^2 surface without a sharply defined minimum. Values of χ^2 greater than one have a positive correlation with increasing error in the angle determinations. This is a valuable property, as it allows one to use the magnitude of χ^2 to flag those rare instances where a poor determination of the patient orientation has been made.

The correlation between χ^2 and the magnitude of rotation around each axis is displayed in Fig. **15**. For the α and β rotations there is no apparent correlation, which indicates that the algorithm's precision and reliability is uniform over the full range of allowable orientations around these axes. The plot for the γ rotations shows greater difficulty in establishing orientation in one of the two directions.

APPLICATIONS

The therapy beam alignment method described in the present invention can be used to direct radiation beams to any part of the body containing radiographic features. In addition, it is obvious that this method may also be used to align instruments other than radiation beams with objects other than disease regions of a patient's body. For example, this method would allow precise positioning of fabrication tools with respect to a manufactured object.

Thus, it is obvious that modifications and variations of the present invention are possible. Therefore, it is to be understood that the scope of the invention should be based on the following claims.

CLAIMS

What is claimed is:

1. A method of aligning a plurality of radiation therapy beams with a treatment target of a patient, comprising the steps of:

a) preprocessing, comprising the steps of:

1) conducting a computed tomography (CT) scan; and

2) assembling an intermediate 3-D image from said scan; and

b) treatment, comprising the steps of:

1) acquiring a set of at least two real images of position of said treatment target of a patient;

2) using said at least two real images to produce a first feature vector;

3) generating a set of at least two digitally reconstructed images (DRRs) from said intermediate 3-D image;

4) using said set of at least two digitally reconstructed images to produce a second feature vector;

5) calculating a difference between said first feature vector and said second feature vector; and

6) if said difference does not fall below a minimum allowable value, employing an algorithm to adjust positions of said radiation therapy beams such that said radiation therapy beams are aligned with said treatment target of said patient.

2. The method of claim 1 comprising repeating steps b) 1-6.

3. The method of claim 1, including the step of generating key pixels associated with anatomical edge features.

4. The method of claim 3, including the step of generating a mask for said at least two real images and said at least two digitally reconstructed images by highlighting key pixels.

5. The method of claim 3, wherein said feature vectors are determined by said key pixels.

6. The method of claim 1, using a preprocessing coordinate system and a treatment coordinate system.

7. The method of claim 6, using said preprocessing coordinate system wherein said treatment target of said patient is fixed.

8. The method of claim 6, using said treatment coordinate system wherein said treatment target of said patient is rotated and translated.

9. The method of claim 6 wherein said preprocessing coordinate system and said treatment coordinate system are related by a transformation equation.

10. The method of claim 1, allowing six degrees of freedom of position of said treatment target of said patient.

11. The method of claim 10, wherein said six degrees of freedom include translation measurements.

12. The method of claim 10, wherein said six degrees of freedom include rotational measurements.

13. The method of claim 1, wherein said difference between said vectors is determined by use of chi squared.

14. The method of claim 1, wherein said algorithm provides minimization of chi squared until convergence with said minimum allowable value.

15. The method of claim 14, including the step of adjusting patient anatomy in said intermediate 3-D image.

16. The method of claim 14, including the step of repositioning a camera model responsible for taking said at least two reconstructed images.

17. The method of claim 16, wherein repositioning of said camera model is guided by a lookup table.

18. The method of claim 17, wherein said lookup table provides the first derivative of said translation and rotation measurements.

19. The method of claim 14, wherein coordinates of repositioned said camera model are transformed into coordinates for alignment of said radiation therapy beams.

20. The method of claim 14, wherein coordinates of repositioned said camera are transformed into coordinates of alignment of said treatment target of said patient.

21. A method of aligning radiation therapy beams with a treatment target of a patient, comprising the steps of:

a) acquiring a plurality of current two-dimensional images indicative of a current position of said treatment target relative to a means for generating said therapy beams;

b) from a three-dimensional image comprising said treatment target, generating a corresponding plurality of reference two-dimensional images indicative of a reference position of said treatment target relative to said means for generating said therapy beams, wherein said treatment target is aligned with said means for generating said therapy beams in said reference position;

c) comparing current feature vectors defined by said current two-dimensional images with corresponding reference feature vectors defined by said reference two-dimensional images;

d) adjusting said current position if said current feature vectors do not match said reference feature vectors; and

e) applying said therapy beams if said current feature vectors match said reference feature vectors.

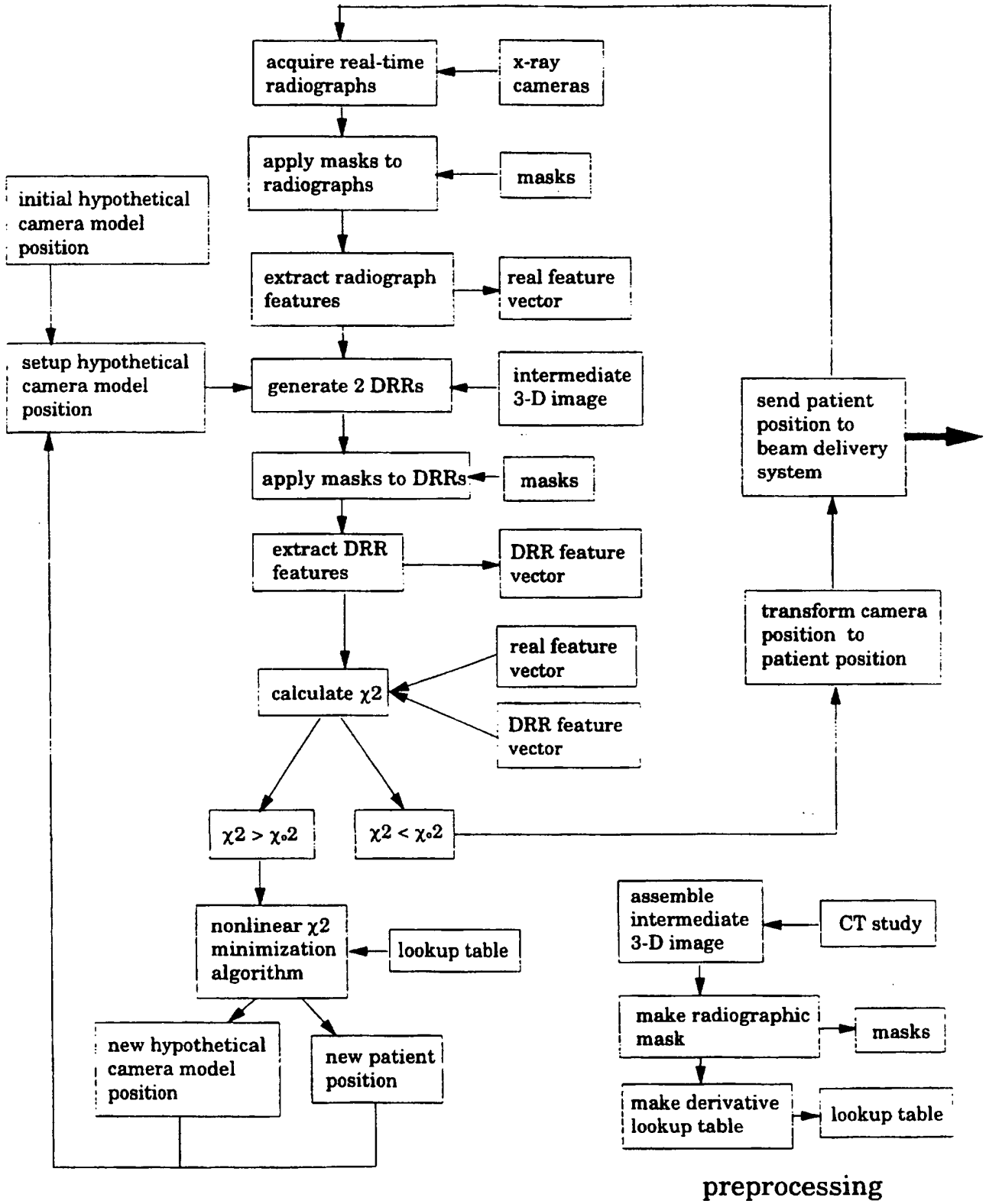
acquire real-time radiographs
x-ray cameras
apply masks to radiographs
masks
initial hypothetical camera model position
extract radiograph features
real feature vector
setup hypothetical camera model position
generate 2 DRRs
intermediate 3-D image
send patient position to beam delivery system
apply masks to DRRs
masks
extract DRR features
DRR feature vector
transform camera position to patient position
real feature vector
calculate χ2
DRR feature vector
χ2 > χ₀2
χ2 < χ₀2
assemble intermediate 3-D image
CT study
nonlinear χ2 minimization algorithm
lookup table
make radiographic mask
masks
new hypothetical camera model position
new patient position
make derivative lookup table
lookup table
preprocessing

FIG. 1

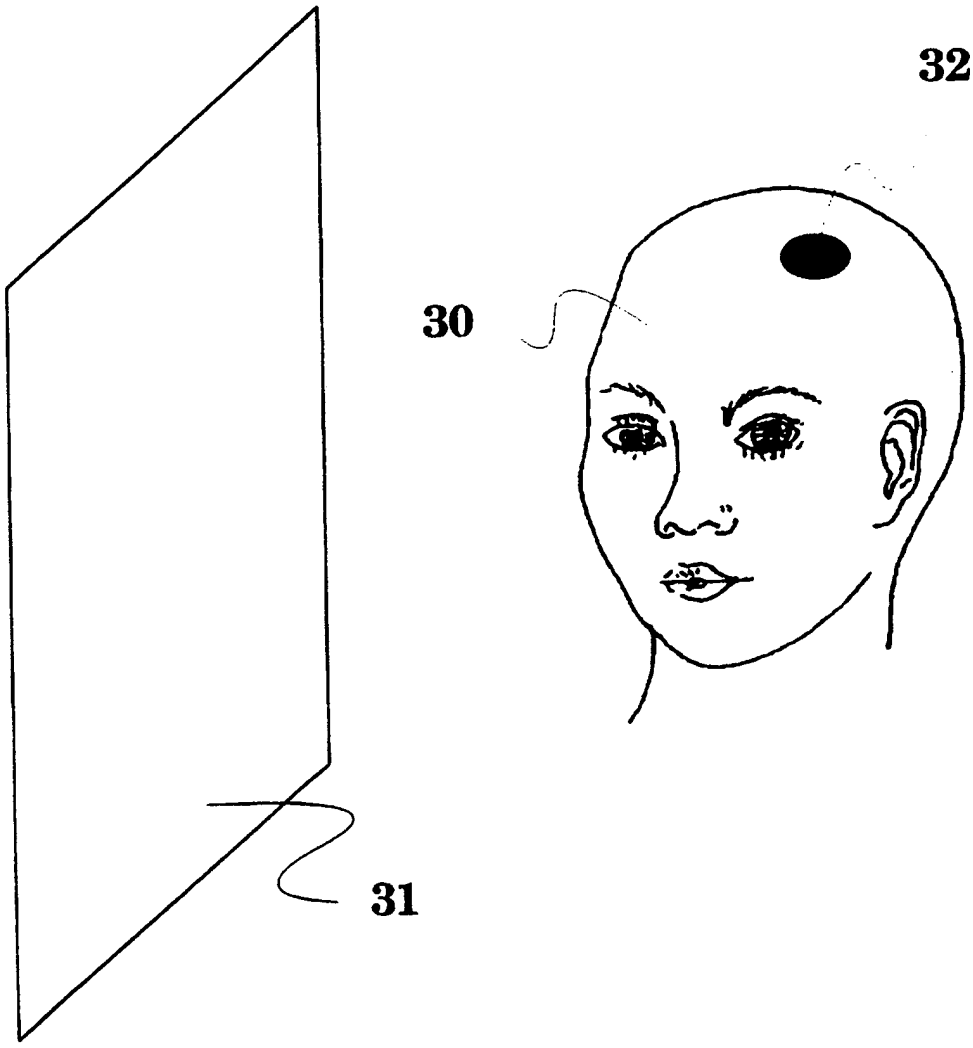

FIG. 2

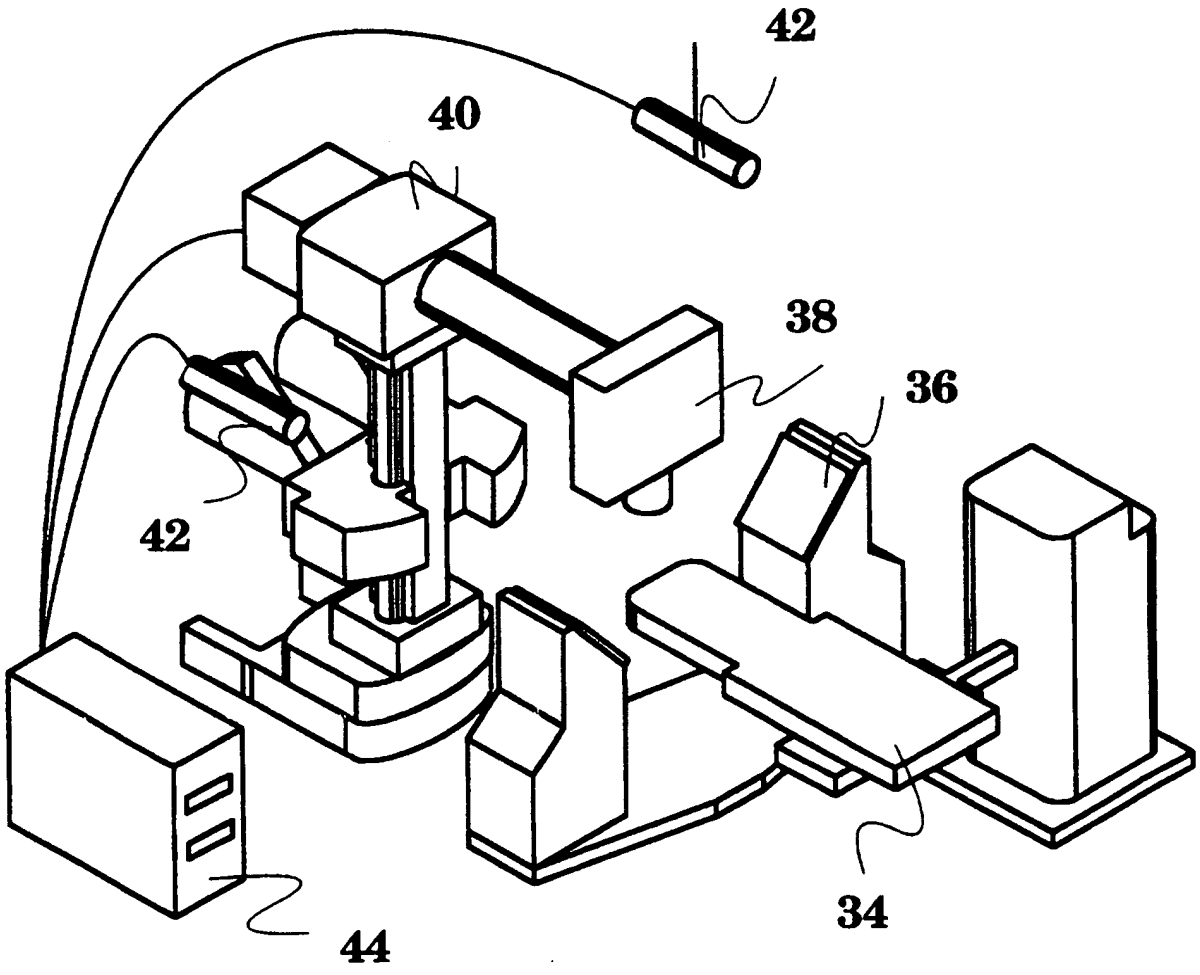

FIG. 3

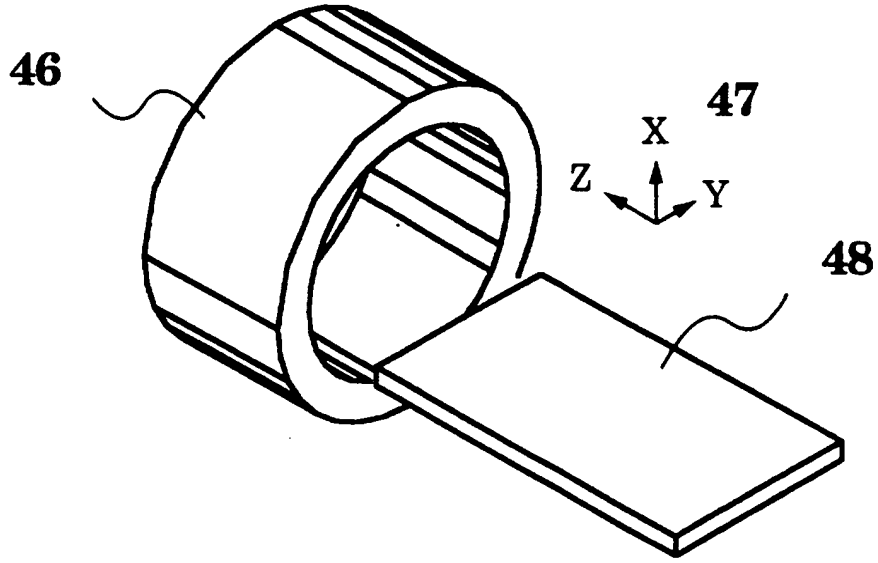

FIG. 4

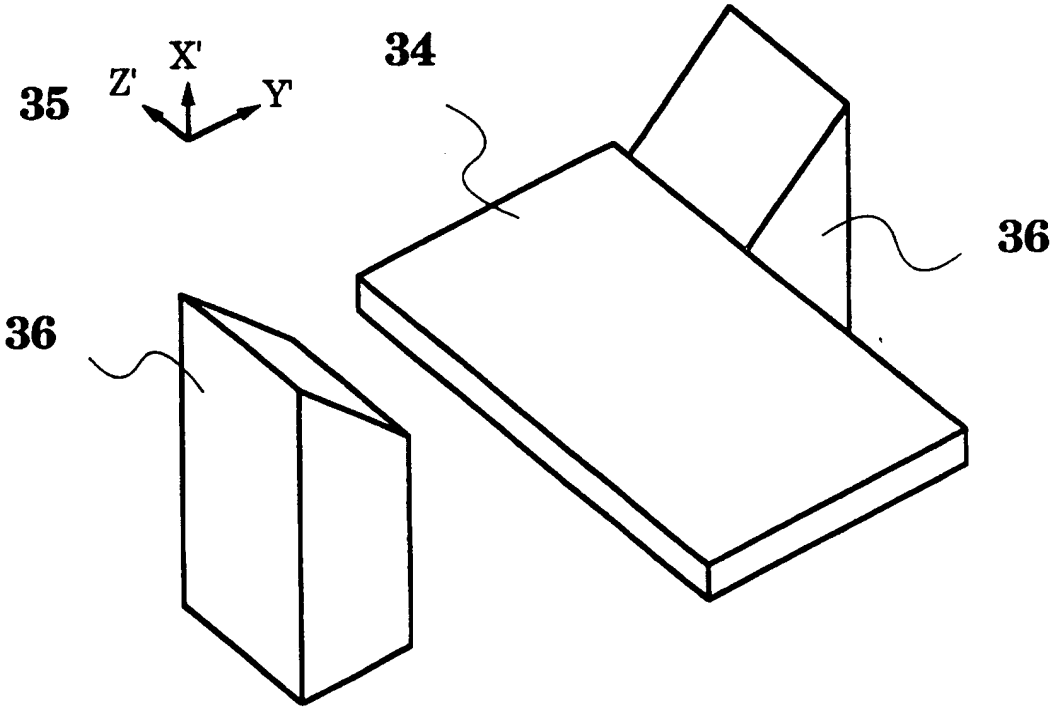

FIG. 5

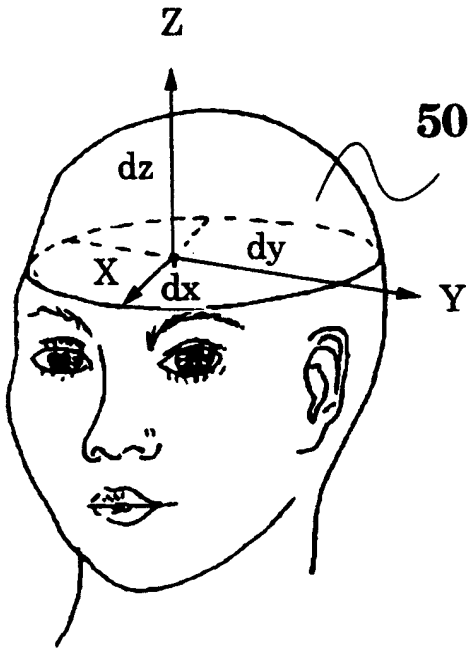

FIG. 6

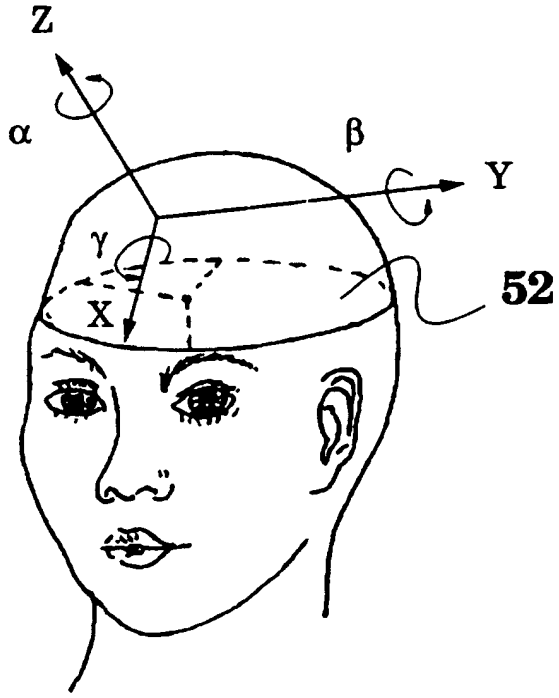

FIG. 7

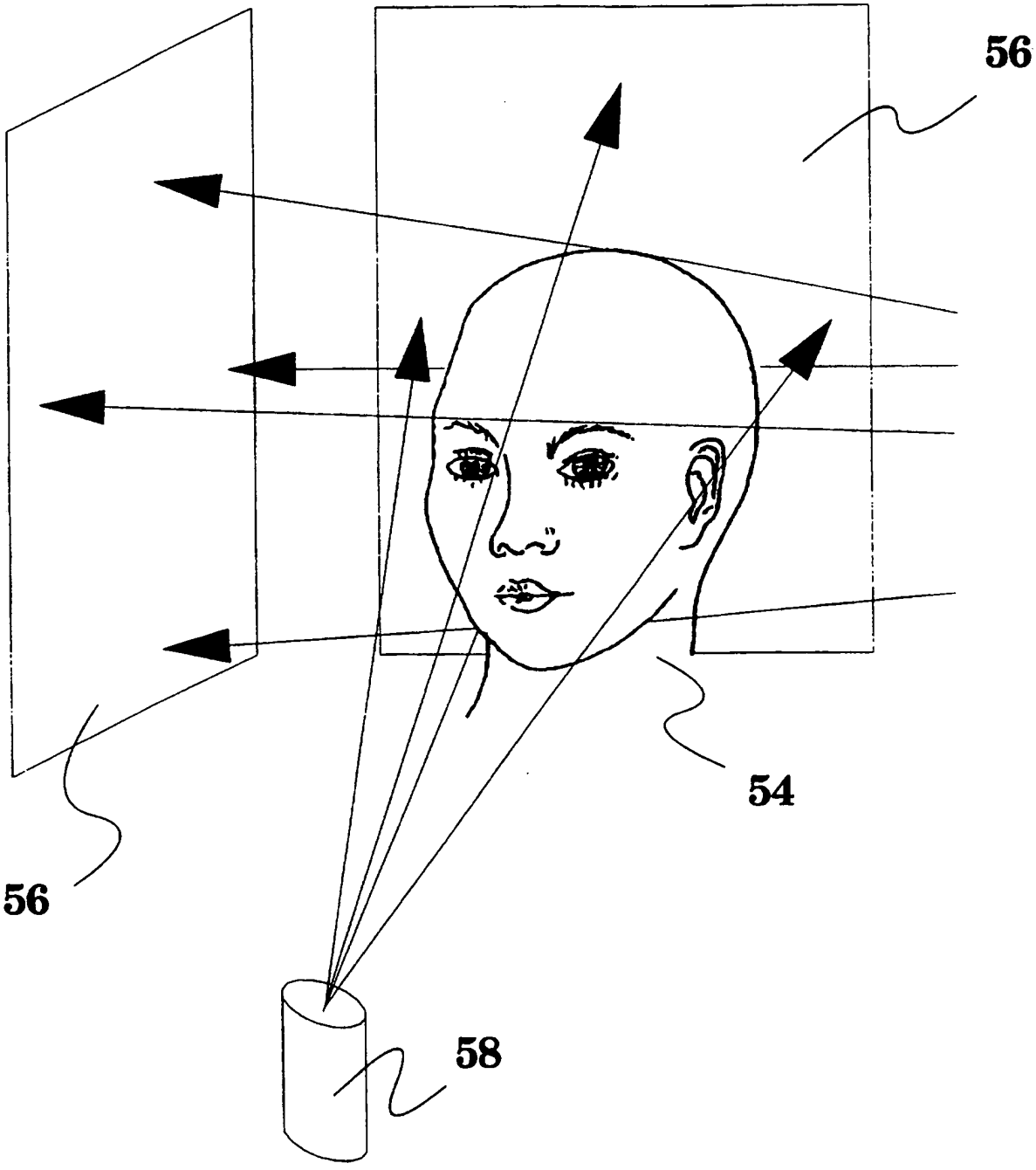

FIG. 8

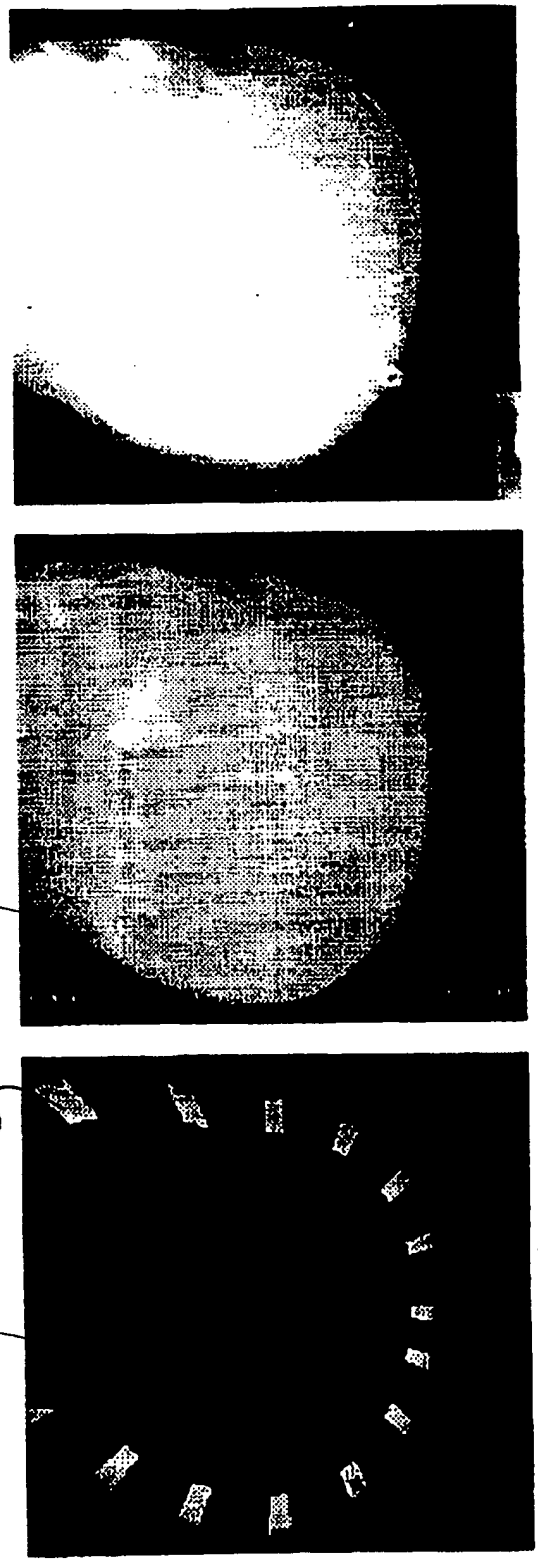

FIG. 9

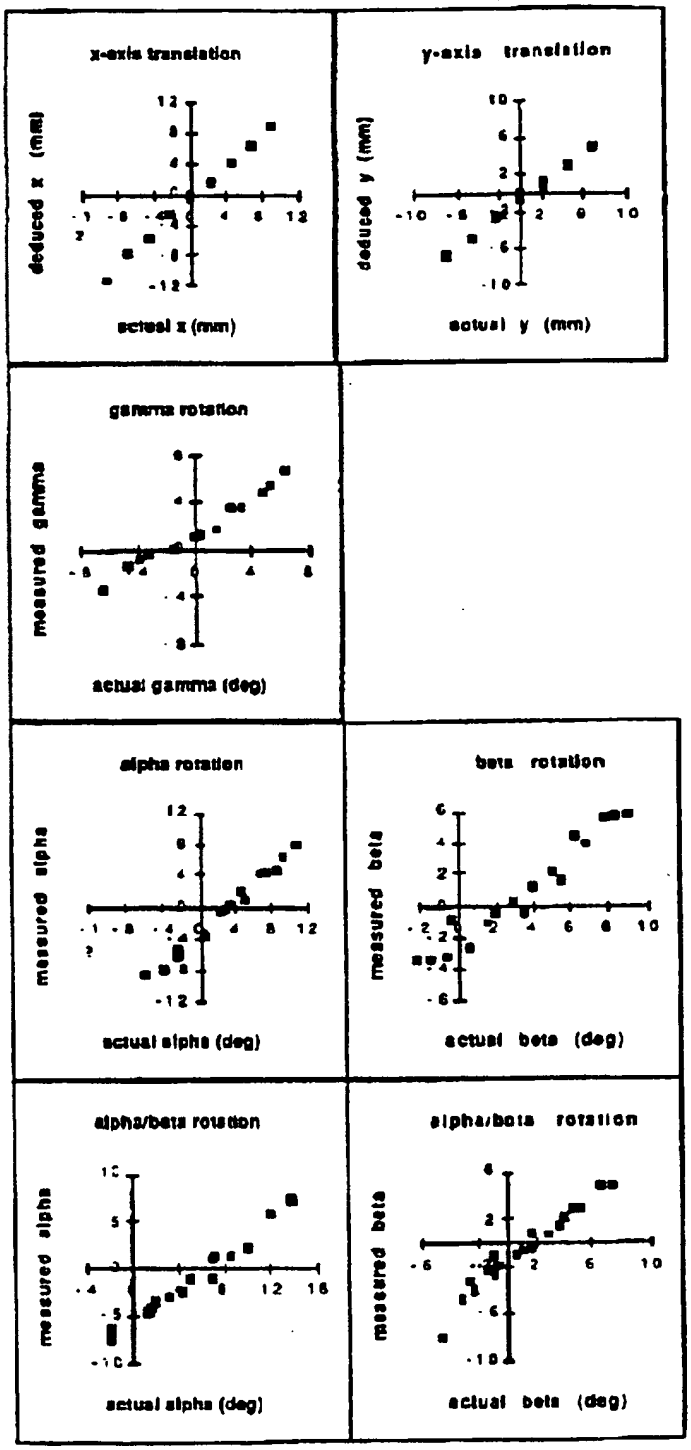
x-axis translation
deduced x (mm)
actual x (mm)
y-axis translation
deduced y (mm)
actual y (mm)
gamma rotation
measured gamma
actual gamma (deg)
alpha rotation
measured alpha
actual alpha (deg)
beta rotation
measured beta
actual beta (deg)
alpha/beta rotation
measured alpha
actual alpha (deg)
alpha/beta rotation
measured beta
actual beta (deg)

FIG. 10

Fits of the deduced versus actual phantom position data to straight lines and standard deviations σ

single component motion	two parameter fit slope	σ	one parameter fit slope	σ
x	1.05 ± 0.05	0.5 mm	1.00	0.6
y	0.73 ± 0.07	0.5 mm	1.00	1.0
α	1.03 ± 0.04	0.67°	1.00	0.67°
β	0.93 ± 0.05	0.82°	1.00	0.92°
γ	0.77 ± 0.05	0.54°	1.00	1.37°
composite motion				
α	0.89 ± 0.03	0.71°	1.00	1.01°
β	0.91 ± 0.05	0.79°	1.00	0.85°

FIG. 11

FIG. 12

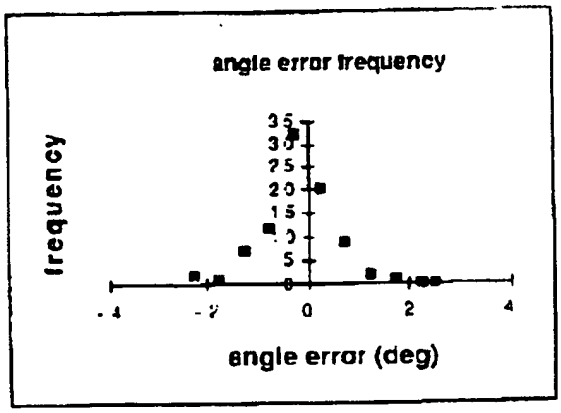

FIG. 13

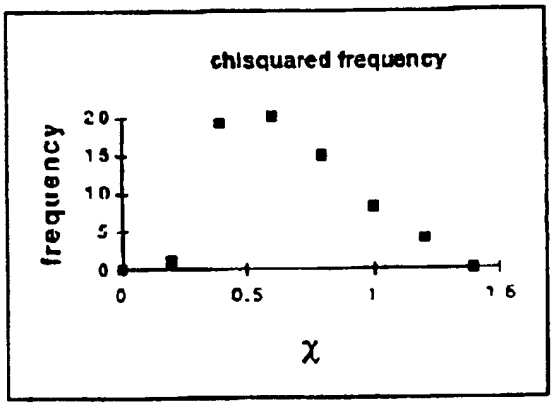

FIG. 14

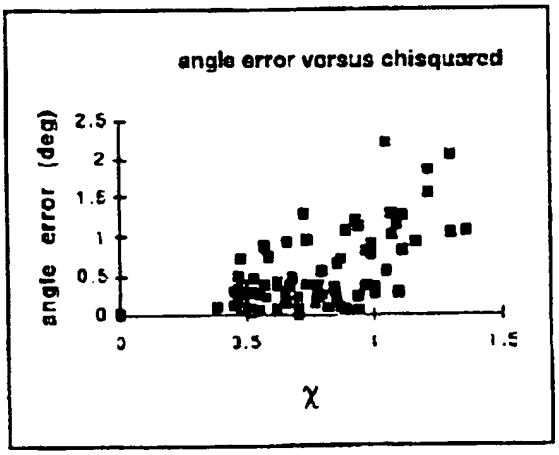

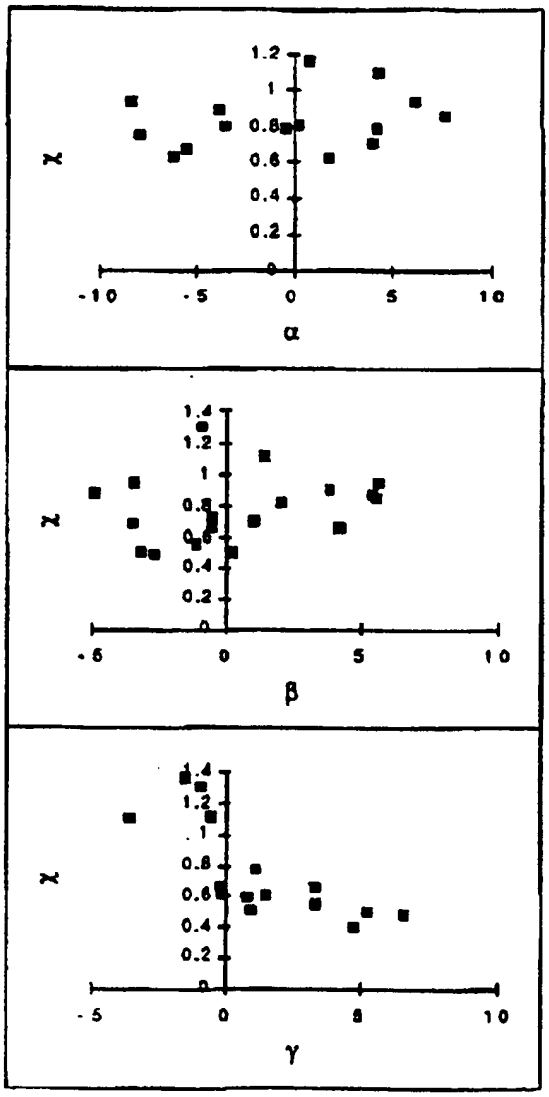
χ
1.2
1
0.8
0.6
0.4
0.2
0
-10
-5
0
5
10
α
χ
1.4
1.2
1
0.8
0.6
0.4
0.2
0
-5
0
5
10
β
χ
1.4
1.2
1
0.8
0.6
0.4
0.2
0
-5
0
5
10
γ

FIG. 15

INTERNATIONAL SEARCH REPORT

International application No.
PCT/US97/11592

A. CLASSIFICATION OF SUBJECT MATTER

IPC(6) :A61B 5/05
US CL :600/407
According to International Patent Classification (IPC) or to both national classification and IPC

B. FIELDS SEARCHED

Minimum documentation searched (classification system followed by classification symbols)

U.S. : 378/63-65; 600/407; 606/130

Documentation searched other than minimum documentation to the extent that such documents are included in the fields searched

Electronic data base consulted during the international search (name of data base and, where practicable, search terms used)

C. DOCUMENTS CONSIDERED TO BE RELEVANT

Category*	Citation of document, with indication, where appropriate, of the relevant passages	Relevant to claim No.
A	US 5,117,829 A (MILLER et al.) 02 June 1992, entire document.	1-21
A	US 4,998,268 A (WINTER) 05 March 1991, entire document.	1-21
A	US 5,418,827 A (DEASY et al.) 23 May 1995, entire document.	1-21

☐ Further documents are listed in the continuation of Box C. ☐ See patent family annex.

*	Special categories of cited documents:	"T"	later document published after the international filing date or priority date and not in conflict with the application but cited to understand the principle or theory underlying the invention
"A"	document defining the general state of the art which is not considered to be of particular relevance	"X"	document of particular relevance; the claimed invention cannot be considered novel or cannot be considered to involve an inventive step when the document is taken alone
"E"	earlier document published on or after the international filing date	"Y"	document of particular relevance; the claimed invention cannot be considered to involve an inventive step when the document is combined with one or more other such documents, such combination being obvious to a person skilled in the art
"L"	document which may throw doubts on priority claim(s) or which is cited to establish the publication date of another citation or other special reason (as specified)	"&"	document member of the same patent family
"O"	document referring to an oral disclosure, use, exhibition or other means		
"P"	document published prior to the international filing date but later than the priority date claimed		

Date of the actual completion of the international search 26 OCTOBER 1997	Date of mailing of the international search report 17 NOV 1997
Name and mailing address of the ISA/US Commissioner of Patents and Trademarks Box PCT Washington, D.C. 20231 Facsimile No. (703) 305-3230	Authorized officer BRIAN E. CASLER Telephone No. (703) 308-3552

Form PCT/ISA/210 (second sheet)(July 1992)*

This Page is Inserted by IFW Indexing and Scanning Operations and is not part of the Official Record

BEST AVAILABLE IMAGES

Defective images within this document are accurate representations of the original documents submitted by the applicant.

Defects in the images include but are not limited to the items checked:

- ☐ BLACK BORDERS
- ☐ IMAGE CUT OFF AT TOP, BOTTOM OR SIDES
- ☑ FADED TEXT OR DRAWING
- ☐ BLURRED OR ILLEGIBLE TEXT OR DRAWING
- ☐ SKEWED/SLANTED IMAGES
- ☐ COLOR OR BLACK AND WHITE PHOTOGRAPHS
- ☑ GRAY SCALE DOCUMENTS
- ☐ LINES OR MARKS ON ORIGINAL DOCUMENT
- ☐ REFERENCE(S) OR EXHIBIT(S) SUBMITTED ARE POOR QUALITY
- ☐ OTHER: _____

IMAGES ARE BEST AVAILABLE COPY.

As rescanning these documents will not correct the image problems checked, please do not report these problems to the IFW Image Problem Mailbox.